Published in final edited form as:
Oncogene. 2013 August 15; 32(33): 3819–3828. doi:10.1038/onc.2012.406.

The epigenetic regulator UHRF1 promotes ubiquitination-mediated degradation of the tumor-suppressor protein promyelocytic leukemia protein

D Guan[1], **D Factor**[1], **Yu Liu**[1], **Z Wang**[2,3], and **H-Y Kao**[1,3]

[1]Department of Biochemistry and Case Western Reserve University, Cleveland, OH, USA

[2]Department of Genetics, Case Western Reserve University School of Medicine, Cleveland, OH, USA

[3]The Comprehensive Cancer Center of Case Western Reserve University and University Hospitals of Cleveland, Cleveland, OH, USA

Abstract

The promyelocytic leukemia (PML) protein is a tumor suppressor originally identified in acute promyelocytic leukemia and implicated in tumorigenesis in multiple forms of cancer. Here, we demonstrate that the PML protein undergoes ubiquitination-mediated degradation facilitated by an E3 ligase UHRF1 (ubiquitin-like with PHD and RING finger domains 1), which is commonly upregulated in various human malignancies. Furthermore, UHRF1 negatively regulates PML protein accumulation in primary human umbilical vein endothelial cells (HUVECs), HEK 293 cells and cancer cells. Knockdown of UHRF1 upregulates whereas ectopic overexpression of UHRF1 downregulates protein abundance of endogenous or exogenous PML, doing so through its binding to the N-terminus of PML. Overexpression of wild-type UHRF1 shortens PML protein half-life and promotes PML polyubiquitination, whereas deletion of the RING domain or coexpression of the dominant-negative E2 ubiquitin-conjugating enzyme, E2D2, attenuates this modification to PML. Finally, knockdown of UHRF1 prolongs PML half-life and increases PML protein accumulation, yet inhibits cell migration and *in vitro* capillary tube formation, whereas co-knockdown of PML compromises this inhibitory effect. These findings suggest that UHRF1 promotes the turnover of PML protein, and thus targeting UHRF1 to restore PML-mediated tumor suppression represents a promising, novel, anticancer strategy.

Keywords

UHRF1; PML; ubiquitination; cell migration; capillary tube formation

INTRODUCTION

The epigenetic regulator UHRF1 (ubiquitin-like with PHD and RING finger domains 1) harbors multiple predicted functional elements, including N-terminal Ub-like, tudor, PHD, SRA and RING domains. By binding to hemimethylated DNA, UHRF1 is known to

Correspondence: Dr H-Y Kao, Department of Biochemistry and Case Western Reserve University, 10900 Euclid Avenue, Cleveland, OH 44106, USA. hxk43@cwru.edu.

CONFLICT OF INTEREST

The authors declare no conflict of interest.

Supplementary Information accompanies the paper on the Oncogene website (http://www.nature.com/onc)

maintain genomic DNA methylation by recruiting DNA methyltransferase, DNMT1, to DNA replication forks.[1–4] Moreover, UHRF1 epigenetically regulates gene transcription by coordinating with histone deacetylase 1,[5] binding to methylated histones[6,7] and promoting histone ubiquitination.[8] However, the role of UHRF1 in genome-independent processes has not been rigorously explored.

UHRF1 is upregulated in several cancers, including breast,[9,10] lung,[11,12] colorectal,[13–15] prostate[16,17] and bladder cancer,[18,19] suggesting that UHRF1 plays a role in carcinogenesis, and is a putative anticancer target. In tumor cells, UHRF1 represses the transcription of several tumor-suppressor genes including *p16INK4A*, *hMLH1*, *p21* and *RB*.[5,20,21] Downregulation of UHRF1 is associated with re-expression of tumor-suppressor genes.[22–24] In addition to its role in epigenetics, we previously reported that UHRF1 promotes DNMT1 ubiquitination and degradation.[14] Intriguingly, overexpression of a RING domain deletion mutant of UHRF1 that lacks E3 ligase activity sensitizes A549 lung cancer cells to treatment with various chemotherapeutics.[8] This finding suggests that the UHRF1 RING domain is a critical functional domain involved in cancer cell proliferation and antiapoptotic activity, and that the RING domain targets tumor-suppressor proteins for degradation. However, the mechanism by which UHRF1 regulates tumor-suppressor proteins remains unresolved.

The promyelocytic leukemia protein (PML) was first isolated as a fusion partner of the retinoic acid receptor-α associated with acute promyelocytic leukemia.[25] It was later demonstrated that PML is a tumor-suppressor protein capable of promoting apoptosis, inhibiting proliferation and inducing senescence.[26] Moreover, we recently identified PML as a negative regulator of cell migration.[27] PML protein is frequently downregulated in various cancers, but PML mRNA levels are relatively similar between normal and cancerous tissues.[28] These observations indicate that PML protein levels are tightly regulated, particularly through posttranscriptional modification. Indeed, several E3 ligases including Siah2,[29] Vmw110/ICP0,[30] E6AP,[31] KLHL20[32] and RNF4[33,34] promote PML ubiquitination and degradation. We have also reported that the peptidylprolyl *cis*/*trans* isomerase Pin1 promotes PML degradation through a phosphorylation-dependent mechanism.[35]

The observations that UHRF1 is upregulated whereas PML protein is downregulated in cancers suggested that UHRF1 may regulate PML protein accumulation. In this study, we identify a novel interaction between PML and UHRF1, and demonstrate that UHRF1 negatively regulates PML by targeting it for ubiquitin-mediated degradation. We further demonstrate that UHRF1 promotes endothelial cell (EC) migration and capillary tube formation, in part by downregulating PML protein levels. Our results support a model in which the E3 ligase activity of UHRF1 promotes PML protein turnover to regulate EC migration and capillary tube formation.

RESULTS

UHRF1 negatively regulates PML protein levels

To determine whether UHRF1 regulates PML protein accumulation, UHRF1 was transiently knocked down using two different UHRF1 small interfering RNAs (siRNAs) in human umbilical vein endothelial cells (HUVECs). We found that knockdown of UHRF1 by siRNAs resulted in an increase in endogenous PML protein accumulation (Figure 1A) without having an effect on its mRNA levels (Figure 1B). The multiple bands present in the PML blot represent the various isoforms of PML and their post-translationally modified derivatives.[36] When compared with the scramble siRNA, UHRF1 knockdown led to an increase in most PML isoforms. This observation was accompanied by an increase in the number of PML nuclear bodies (Figures 1C, top row, and 1D). In contrast, overexpression of hemagglutinin (HA)-UHRF1 significantly decreased endogenous PML levels

(Supplementary Figure 1), whereas the enzymatically defective mutants, C741A or ΔRing,[16] had only a minor effect (Figure 1E). These data indicate that UHRF1 negatively regulates endogenous PML protein levels post-transcriptionally in HUVECs.

We further examined whether this regulation extends to other cell types. HEK 293 cells (human embryonic kidney 293 cells) and HeLa cells were co-transfected with FLAG-PML4 and green fluorescent protein (GFP; as a loading control), with or without HA-UHRF1. Cells transfected with HA-UHRF1 expressed lower levels of FLAG-PML protein than cells transfected with vector (Figures 2a and b). It has been reported that the herpes virus-associated ubiquitin-specific protease HAUSP (or USP7) stabilizes UHRF1 and that knockdown of HAUSP decreases UHRF1 protein levels.[37,38] Indeed, we observed a modest decrease in endogenous UHRF1 protein accumulation when HAUSP is knocked out in DLD1 colon cancer cells. This observation is accompanied by an increase in endogenous PML protein abundance (Figure 2c). Furthermore, ectopic expression of HA-UHRF1 partially abrogates this effect on PML accumulation. We therefore conclude that UHRF1 is capable of downregulating PML protein levels in several cell types.

UHRF1 interacts with PML

To elucidate the potential mechanism by which UHRF1 negatively regulates PML, we characterized the association of UHRF1 and PML using glutathione *S*-transferase (GST) pulldown assays. Immobilized, purified, GST-UHRF1 fusion protein was incubated with cell extracts expressing three commonly studied PML splice isoforms: PML1, PML4 or PML6. We found that GST-UHRF1 was capable of pulling down all three PML isoforms (Figures 3a–c). This interaction was validated by reciprocal coimmunoprecipitation when FLAG-PML6 was transfected with or without HA-UHRF1 (Figure 3d). Furthermore, we carried out coimmunoprecipitation with extracts prepared from HUVECs and found that endogenous PML and endogenous UHRF1 interact (Figure 3e). Therefore, we conclude that UHRF1 and PML physically associate in mammalian cells.

We also determined whether UHRF1 negatively regulates PML protein levels in other cancer cells. We carried out coimmunoprecipitation and found that PML antibodies coprecipitate UHRF1 in PC3 prostate cancer cells, indicating that endogenous PML and UHRF1 interact (Figure 4a). Moreover, knockdown of endogenous UHRF1 increased PML protein accumulation (Figure 4b), but did not alter PML mRNA levels. Similar to that observed in HEK 293 cells, overexpression of wild-type UHRF1 significantly decreased PML protein levels. However, the ligase activity-defective UHRF1 (ΔRing) mutant only modestly decreased PML protein levels. These data indicate that UHRF1 negatively regulates PML protein accumulation in PC3 prostate cancer cells.

Mapping of interaction domains

PML contains RING, B-box 1, B-box 2 and coiled-coil (CC) domains (Figure 5a). To map the interaction of UHRF1 and PML, we performed immunoprecipitation experiments. We found that individual deletions of each domain of PML did not significantly reduce the interaction between PML and UHRF1 in HEK 293 cells (Figure 5b). This observation was further confirmed by GST pull-down assays, although deletion of the B-box 2 or CC domains displayed somewhat decreased PML binding to UHRF1 (Figure 5c). Further mapping by coimmunoprecipitation and GST pull-down assays demonstrated that UHRF1 interacts independently with amino acids 2–180 and 181–350 of PML (Figures 5d and e). In contrast, GST-FLNB (R11-15) fusion protein does not interact with these two domains (Supplementary Figure 2). Together, these data indicate that UHRF1 binds two separate regions of the PML protein.

UHRF1-mediated downregulation of PML protein levels requires B-box 2 and CC domains of PML

To further elucidate the mechanism by which UHRF1 down-regulates PML protein levels, we tested whether UHRF1 regulates PML protein half-life. Our data show that knockdown of UHRF1 resulted in a longer half-life of endogenous PML protein in HUVECs (Figures 6a–d and Supplementary Figure 3). As shown in Figure 5c, deletion of B-box 2 or the CC domain of PML resulted in a decreased association of PML with UHRF1. To determine whether B-box 2 or the CC domain plays a role in UHRF1-mediated PML protein degradation, we examined whether deletion of B-box 2 or the CC domain has an effect on PML protein stability. Wild-type PML, PML (ΔB-box 2) or PML (ΔCC) were transiently transfected into HeLa cells followed by half-life measurements. We found that deletion of B-box 2 or CC domain led to a longer half-life of PML protein, though B-box 2 deletion has a much stronger effect than the CC domain deletion (Figures 6e–h).

We reasoned that if the physical association between PML and UHRF1 plays a role in UHRF1-mediated PML degradation, we anticipate that the half-lives of PML (ΔB-box 2) and PML (ΔCC) should not be affected by UHRF1 knockdown. Indeed, although whereas transfected wild-type PML protein is significantly stabilized in UHRF1 knockdown cells, the half-lives of PML (ΔB-box 2) or PML (ΔCC) are comparable in control and UHRF1 knockdown cells (Figures 6i–k and Supplementary Figure 4). These data indicate that the interaction between PML and UHRF1 is critical for UHRF1-mediated PML protein turnover.

UHRF1 promotes degradation of PML via polyubiquitination UHRF1 possess a C-terminal RING domain that is thought to promote protein ubiquitination. Indeed, we have previously shown that UHRF1 promotes ubiquitination-mediated DMNT1 degradation.[14] To determine whether the RING domain of UHRF1 is essential for the UHRF1-mediated decrease of PML protein levels, HEK 293 cells were co-transfected with HA-PML4 and GFP, with or without wild-type FLAG-UHRF1, or a RING domain deletion mutant. As shown in Figure 7a, wild-type UHRF1 (lane 1) was capable of decreasing HA-PML4 protein abundance. However, E3 ligase-defective mutants ΔRing (lane 3) or the point mutant C741A (lane 4) did not or only slightly decreased PML protein levels, respectively. We further determined whether UHRF1 promotes PML ubiquitination. Cells were transiently transfected with HA-PML4, wild-type or RING domain deletion mutant with or without FLAG-tagged ubiquitin (FLAG-Ub) or a dominant-negative E2D2. The ubiquitin-conjugating enzyme E2D2 has been shown to play a role in UHRF1-mediated ubiquitination.[8,39] Cells were treated with MG132 4 h before harvest followed by immunoprecipitation with anti-HA antibody-conjugated beads and immunoblotting with anti-FLAG or anti-HA antibodies. As shown in Figure 7b, in the absence of exogenous UHRF1, modest levels of PML ubiquitination was detected. This basal level is because of endogenous UHRF1 and other PML E3 ubiquitin ligases. However, ectopically expressed wild-type Myc-UHRF1 (lane 2 vs lane 1), but not the RING domain deletion mutant (lane 3 vs lane 1), potently increased HA-PML4 ubiquitination. Consistent with this notion, the dominant-negative Myc-tagged E2D2 (Myc-dnE2D2) abrogated UHRF1-mediated PML4 ubiquitination. Together, these data indicate that E2D2 and UHRF1 promote ubiquitination-mediated PML degradation.

UHRF1 promotes HUVEC migration and capillary tube formation We have previously demonstrated that PML negatively regulates cell migration.[27] Therefore, we hypothesize that knockdown of UHRF1 will inhibit cell migration, in part, as a result of increased PML protein accumulation. Indeed, siRNA-mediated UHRF1 knockdown resulted in a significant inhibition of HUVEC cell migration as determined by a wound-healing assay (Figure 8). To further evaluate the role of PML in UHRF1 knockdown-mediated inhibition of cell migration, we determined the effects of a double knockdown of UHRF1 and PML on cell

migration. We found that similar to that shown in Figure 1, PML protein accumulated in UHRF1 knockdown cells (Figure 9a). Accordingly, wound-healing assays showed that cell migration was inhibited upon UHRF1 knockdown (Figure 9b, samples siU-1 and siU-2), mirroring the results shown in Figure 8. However, this inhibition was largely relieved by co-knockdown of PML (Figure 9b, samples siU-1/siPML and siU-2/siPML). This result was further confirmed by transwell migration assays (Figure 9c). Additionally, we carried out *in vitro* capillary tube formation assays, and found that knockdown of UHRF1 significantly reduced tube formation, whereas further knockdown of PML ablated the inhibitory effect of UHRF1 knockdown (Figure 9d). In summary, these data strongly suggest that UHRF1 promotes HUVEC migration and capillary tube formation, in part by downregulating PML protein accumulation.

DISCUSSION

UHRF1 is best known as an epigenetic regulator because of its ability to modulate heterochromatin by binding hemimethylated CpG dinucleotides,[4] unmethylated histone H3R2[40] and H3K4me0/K9me3.[41] Our present study identifies a novel UHRF1 target, PML, and, conversely, a novel E3 ubiquitin ligase for PML. We demonstrate that UHRF1 interacts with PML to modulate its protein stability. Furthermore, we show that the C-terminal RING domain is essential to promote ubiquitination-mediated degradation of PML, thereby providing a novel mechanism by which UHRF1 might promote tumorigenesis.

Recent immunohistochemical staining and microarray analyses from various cancer patients indicate that UHRF1 is overexpressed in several cancer types but not in normal cells.[11,12,18,42,43] Although its role in tumorigenesis is thought to involve promotion of cell proliferation and metastasis,[12,13] the underlying mechanism is still elusive. Conversely, the tumor-suppressor protein PML, which inhibits cell cycle progression and promotes apoptosis, is found to be downregulated in cancer cells, whereas its mRNA level remains unchanged.[28] Interestingly, it was reported that a RING domain deletion UHRF1 mutant that lacks E3 ligase activity inhibits A549 lung cancer cell growth.[16] This observation implies a critical role of the UHRF1 E3 ligase activity in the promotion of tumorigenesis. Therefore, identification of UHRF1 E3 ligase targets provides a promising avenue for elucidating the mechanism by which UHRF1 promotes tumorigenesis. In this study, we show that overexpression of the E3 ligase-defective (RING domain deletion) UHRF1 mutant or a dominant-negative E2D2 ubiquitin-conjugating enzyme significantly inhibited the ability of UHRF1 to promote PML ubiquitination (Figure 7b). Thus, our data support the hypothesis that PML is a critical cellular target of UHRF1 and that over-expression of UHRF1 results in downregulation of PML protein accumulation.

PML is highly expressed in ECs,[44] but its role in ECs remains largely unexplored. We have previously shown that tumor necrosis factor-α induces PML protein expression and promotes sequestration of histone deacetylase 7 to PML nuclear bodies, thereby de-repressing histone deacetylase 7 target genes.[45] We have also recently demonstrated an inhibitory role of PML in EC migration and capillary tube formation.[46] In contrast, the role of UHRF1 in ECs has not been explored. We show here that knockdown of UHRF1 in HUVECs results in an increase in PML protein accumulation without changing its mRNA levels and this increase is associated with reduced cell migration and capillary tube formation. This inhibitory effect is significantly alleviated by further knockdown of PML. These data support a model in which UHRF1 promotes EC migration, invasion and capillary tube formation, in part, by decreasing PML protein abundance.

The herpes virus-associated ubiquitin-specific protease HAUSP positively regulates UHRF1 protein stability by protecting UHRF1 from autoubiquitination,[37] whereas it negatively

regulates PML protein accumulation.[47] These reports raise the possibility that HAUSP decreases PML protein accumulation indirectly by upregulating UHRF1 protein abundance. Our data show that ectopically transfected UHRF1 is capable of decreasing PML protein levels, regardless of the status of HAUSP (Figure 2c). Intriguingly, HAUSP interacts with Vmw110/ICP0, the herpes simplex virus type 1 immediate-early protein,[30] another PML E3 ligase.[47] Similarly, HAUSP blocks ICP0 autoubiquitination[48] and enhances ICP0 protein stability. Taken together, our data suggest that Vmw110/ICP0 is functionally a viral counterpart of the UHRF1 E3 ligase.

PML promotes p53 K382 acetylation, which increases p53-mediated transcriptional activation, in response to oncogenic Ras[49] or ultraviolet (UV) irradiation.[50] To determine whether UHRF1 regulates p53 acetylation and transcriptional activation via PML, we examined the acetylation status of p53 at K382 in UHRF1 single-knockdown and UHRF1/PML double-knockdown HUVECs. Although whereas we were able to detect an increase in the expression of p53 target genes including *p21* and *Gadd45* in UHRF1 knockdown cells, we did not observe changes in p53 K382 acetylation (Supplementary Figure 5). Therefore, the increase in *p21* and *Gadd45* gene expression induced by UHRF1 knockdown is independent of increases in p53 K382 acetylation. Indeed, those two studies[49,50] did not conclude that an increase in PML alone is capable of promoting p53 acetylation. UV-induced p53 acetylation depends on UV-activated HIPK2 kinase activity, which promotes S46 phosphorylation in p53, which in turns promote its acetylation. In addition to their direct effects on PML, both oncogenic Ras and UV irradiation activate downstream signalings and effectors that are independent of PML. Collectively, downstream PML-dependent and -independent signaling is required for Ras and UV-induced increases in p53 K382 acetylation. Consistent with this notion, our data show that knockdown of UHRF1 alone in HUVECs is insufficient to alter p53 acetylation status.

In summary, we have identified UHRF1 as a novel PML E3 ubiquitin ligase and therefore provided the first example by which UHRF1 negatively regulates tumor suppressor at the post-transcriptional level. Identification of other tumor-suppressor proteins, which are downregulated and ubiquitinated by UHRF1, will be essential to fully understand the role of UHRF1 in cancer and to facilitate UHRF1 as a target for cancer therapy.

MATERIALS AND METHODS

Cell lines and medium

HUVECs (C2519A; Lonza Inc, Allendale, NJ, USA) that had undergone less than five passages were used in this study. Cells were maintained in Endothelial Cell Growth Medium-2 (CC-4176; Lonza Inc). HEK 293 and HeLa cells were maintained in Dulbecco's modified Eagle's medium (Cellgro, Mediatech, Inc., Herndon, VA, USA) supplemented with 10% fetal bovine serum and 50 units/ml penicillin and streptomycin sulfate. Wild-type and HAUSP knockout DLD1 cells were grown as described previously.[14] PC3 cells were maintained in F12K medium (Invitrogen, Carlsbad, CA, USA) supplemented with 10% fetal bovine serum.

Plasmid construction and transfection

The UHRF1 expression construct was kindly provided by Dr Christian Bronner (Illkirch Cedex, France) and sub-cloned into the pCMX plasmid. GST-UHRF1 and GST-FLNB (Immunoglobulin-like domain 11-15, R11-15) were constructed by PCR using HA-UHRF1 and HA-FLNB as templates, respectively, and subsequently subcloned into the pGEX4T-1 vector. PML1, PML4 or PML6 were inserted into pCMX-HA or pCMX-FLAG plasmids as described previously.[35] Flag-HAUSP was described previously.[14] Full-length UHRF1 and

different truncations of UHRF1 and PML were generated by PCR and subcloned into pCMX-HA or pCMX-FLAG plasmids. The dominant-negative E2D2, CMX-His-Myc-dnD2E2, was generated by PCR using His-dnE2D2 (kindly provided by Dr Cam Patterson, Chapel Hill, NC, USA) as a template. The UHRF1 mutants, C741A and ΔRing (in which amino acids 724–763 were deleted), were previously described in Jenkins *et al.*[16] and were generated by site-specific PCR mutagenesis and verified by sequencing. Lipofectamine 2000 (Invitrogen) was used for transfection according to the manufacturer's instructions.

Immunofluorescence microscopy

Immunofluorescence microscopy was carried out as described previously,[51] with the following modifications. Primary antibody incubation with anti-PML, anti-UHRF1 was carried out at room temperature for 2 h. After washing, Alexa Fluor secondary antibodies (Invitrogen) were added and incubated for 40 min in the dark. Nuclei were counterstained with 4,6-diamidino-2-phenylindole (Vector Laboratories, Burlingame, CA, USA). All images were captured under the same settings using a Leica immunofluorescence microscope (Leica, Wetzlar, Germany).

siRNA transfection and antibodies

Nontargeting control (D-001810-01), PML (J-006547-05) and UHRF1 (J-006977-05 and J-006977-08) siRNAs and transfection regent DharmaFECT1 (T-2001) were purchased from Thermo Scientific (Rockland, IL, USA). Anti-PML and UHRF rabbit polyclonal antibodies were purified in-house. The following antibodies were purchased: β-actin (A5441) and FLAG (F1084) from Sigma (St Louis, MO, USA); HA-HRP (12013819001) from Roche Applied Science (Indianapolis, IN, USA); rabbit polyclonal anti-PML (sc-5621) and anti-HA (sc-805) and mouse monoclonal anti-PML (sc-966), p53 (sc-126) and anti-GFP (sc-9996) from Santa Cruz Biotechnology (Santa Cruz, CA, USA); rabbit polyclonal anti-p53 acetyl-K382 (no. 2525), mouse monoclonal anti-Myc (no. 2276) from Cell Signaling Technology (Danvers, MA, USA); and mouse monoclonal UHRF1 (612264) from BD Biosciences (San Jose, CA, USA).

RNA isolation and quantitative reverse transcriptase–PCR

HUVECs were transiently transfected with UHRF1 or scramble siRNAs for 72 h and total RNA was isolated using a PrepEase RNA Spin kit (Affymetrix, Santa Clara, CA, USA). Complementary DNAs were generated using iScript Reverse Transcription Supermix kit (Bio-Rad, Richmond, CA, USA) according to the manufacturer's protocol. The specific complementary DNAs of interest were amplified and quantified by real-time PCR using an iCycler (Bio-Rad) platform with 2X IQ SYBR Green Supermix (Bio-Rad) and appropriate primers. The relative quantities of UHRF1 and PML mRNA were normalized to 18S RNA, and shown as means±s.d. from three independent experiments. The primer sequences for quantitative reverse transcriptase–PCR are described in Supplementary Table 1.

Immunoprecipitation and western analysis

HEK 293 cells, transfected with the indicated plasmids, or untreated HUVECs were washed with 1 × phosphate-buffered saline and resuspended in NETN (20 mM Tris–HCl, pH 8.0, 100 mM NaCl, 1 mM EDTA, 10% glycerol, 1 mM dithiothreitol and 0.1% NP-40) buffer along with a protease inhibitor cocktail (Roche Applied Science), followed by sonication to lyse the cells. Lysed cells were centrifuged at 4 °C at 12 000 r.p.m. for 10 min, and the supernatant was incubated with protein A conjugated beads for preclearing. To detect exogenous protein interactions, whole-cell extracts were incubated with anti-HA antibody conjugated beads (F2426; Sigma) or anti-FLAG antibody conjugated beads (E6779; Sigma). For endogenous protein interactions, whole-cell extracts were incubated with anti-PML

antibodies for 3 h and then incubated with protein A conjugated beads for 2 h. The beads were washed with NETN buffer five times, and supernatants were discarded. Then, 2 × sample buffer was added to the beads to elute immunoprecipitated protein, followed by sodium dodecyl sulfate–polyacrylamide gel electrophoresis (SDS–PAGE) and western blotting as previously described.[51]

GST pull-down assay

GST pull-down assays were performed according to a previously published protocol.[52] Purified immobilized GST-UHRF1 fusion protein was incubated with whole-cell extracts from cells expressing the indicated proteins. After incubation, the beads were washed three times with NETN buffer and the supernatant was discarded. Then, 2 × sample buffer was added to elute protein from the beads followed by SDS–PAGE and western blotting.

Determination of endogenous and transfected PML protein half-lives

To determine the half-life of endogenous PML in HUVECs, cells were transiently transfected with a nontargeting siRNA, or two independent UHRF1 siRNAs. After 48 h, cells were trypsinized and equal numbers of cells was plated. After 12 h, cells were treated with cycloheximide (20 μg/ml) for the indicated times. To determine the half-life of transfected PML4, HeLa cells were transiently transfected with UHRF1 with a nontargeting siRNA, or two independent UHRF1 siRNAs. After 24 h, cells were transfected with wild-type or mutant HA-PML4 expression plasmids. Another 24 h later, cells were trypsinized and equal number of cells was plated for 12 h followed by cycloheximide (20 μg/ml) treatment as described above. The half-lives of endogenous and transfected wild-type or mutant PML were determined by western blotting and the intensity of the signals was quantified by ImageJ (Bethesda, MD, USA).

Ubiquitination assay

The ubiquitination assay was performed as described.[53] Briefly, HEK 293 cells were transfected with the indicated plasmids (Figure 7b) and treated with 20 mM MG132 for 4 h before harvest. Cells were lysed with RIPA buffer (20 mM Tris–HCl, pH 7.5, 200 mM NaCl, 1 mM EDTA, 1% Triton X-100, 1 mM dithiothreitol and 0.1% SDS), and lysates were immunoprecipitated using anti-HA antibody conjugated beads (E6779; Sigma) followed by western blotting with anti-FLAG (ubiquitin) antibody to detect PML ubiquitination. After washing, the polyvinylidene difluoride membrane was stripped and incubated with anti-HA antibody to detect PML as the loading control.

Wound-healing assay

HUVECs were transfected with the indicated siRNAs. After 60 h, cells were trypsinized and 10^6 cells were reseeded on a six-well tissue culture plate. After 6 h, the attached cells were scratched with a 200 μl pipette tip and 0 h images were captured using a Leica Wetzlar microscope. The plates were placed back at 37 °C and 5% CO_2 for 8 h, and another set of images were captured of the same wounds. The wound widths were measured by ImageJ (version 1.44, NIH), normalized and presented as the percentage of wound measured at time 0 (mean±s.d.). The percent of migration was calculated as the width of a scratch divided by the initial width of the same scratch times 100. At least five fields were analyzed for each scratch and each sample was performed in duplicate.

Transwell migration assay

At 60 h after transfection by the indicated siRNAs, HUVECs were trypsinized, and 10^5 cells seeded on transwell inserts with 8 μm micropore filters (Corning Costar, Cambridge, MA, USA) in 200 μl medium. Medium containing 10% fetal calf serum was added to the lower

chamber as a chemoattractant. After 12 h, cells on the upper side of the filter were removed with a cotton swab. The remaining cells were fixed and stained using 4,6-diamidino-2-phenylindole, followed by imaging on a Leica immunofluorescence microscope. Five random fields were imaged per transwell insert and the number of cells that had migrated to the bottom side of the membrane was counted using the particle counting module of ImageJ. Each assay was repeated in three independent experiments, resulting in 15 fields for each sample.

In vitro capillary tube formation assay

The assays were performed using a commercially available kit from Millipore (ECM 625, Billerica, MA, USA). The gel matrix was prepared as recommended by the manufacturer, and allowed to solidify in 96-well plate. At 64 h after transfection by the indicated siRNAs, HUVECs were trypsinized, and 5×10^4 cells seeded onto the surface of the polymerized matrix. The plate was incubated at 5% CO_2, 37 °C for 3 or 8 h, and images were captured using a Leica Wetzlar microscope. The branch points were counted and presented as mean ±s.d. Unpaired two-tail *t*-tests were used to determine significance.

Supplementary Material

Refer to Web version on PubMed Central for supplementary material.

Acknowledgments

We thank Dr David Samols for his comments on the manuscript. D Factor is supported by training Grant T32HD07104. This project is supported by the NIH through R01 DK078965, HL093269 and Case Comprehensive Cancer Center Program in Aging and Energy Balance, NCI P20 CA103767 to H-Y Kao and CA127590 to Z Wang.

References

1. Arita K, Ariyoshi M, Tochio H, Nakamura Y, Shirakawa M. Recognition of hemi-methylated DNA by the SRA protein UHRF1 by a base-flipping mechanism. Nature. 2008; 455:818–821. [PubMed: 18772891]
2. Avvakumov GV, Walker JR, Xue S, Li Y, Duan S, Bronner C, et al. Structural basis for recognition of hemi-methylated DNA by the SRA domain of human UHRF1. Nature. 2008; 455:822–825. [PubMed: 18772889]
3. Hashimoto H, Horton JR, Zhang X, Bostick M, Jacobsen SE, Cheng X. The SRA domain of UHRF1 flips 5-methylcytosine out of the DNA helix. Nature. 2008; 455:826–829. [PubMed: 18772888]
4. Bostick M, Kim JK, Esteve PO, Clark A, Pradhan S, Jacobsen SE. UHRF1 plays a role in maintaining DNA methylation in mammalian cells. Science. 2007; 317:1760–1764. [PubMed: 17673620]
5. Unoki M, Nishidate T, Nakamura Y. ICBP90, an E2F-1 target, recruits HDAC1 and binds to methyl-CpG through its SRA domain. Oncogene. 2004; 23:7601–7610. [PubMed: 15361834]
6. Hu L, Li Z, Wang P, Lin Y, Xu Y. Crystal structure of PHD domain of UHRF1 and insights into recognition of unmodified histone H3 arginine residue 2. Cell Res. 2011; 21:1374–1378. [PubMed: 21808300]
7. Xie S, Jakoncic J, Qian C. UHRF1 double tudor domain and the adjacent PHD finger act together to recognize K9me3-containing histone H3 tail. J Mol Biol. 2011; 415:318–328. [PubMed: 22100450]
8. Citterio E, Papait R, Nicassio F, Vecchi M, Gomiero P, Mantovani R, et al. Np95 is a histone-binding protein endowed with ubiquitin ligase activity. Mol Cell Biol. 2004; 24:2526–2535. [PubMed: 14993289]
9. Yan F, Tan XY, Geng Y, Ju HX, Gao YF, Zhu MC. Inhibition effect of siRNA-downregulated UHRF1 on breast cancer growth. Cancer Biother Radiopharm. 2011; 26:183–189. [PubMed: 21539450]

10. Li X, Meng Q, Rosen EM, Fan S. UHRF1 confers radioresistance to human breast cancer cells. Int J Radiat Biol. 2011; 87:263–273. [PubMed: 21067293]
11. Unoki M, Daigo Y, Koinuma J, Tsuchiya E, Hamamoto R, Nakamura Y. UHRF1 is a novel diagnostic marker of lung cancer. Br J Cancer. 2010; 103:217–222. [PubMed: 20517312]
12. Daskalos A, Oleksiewicz U, Filia A, Nikolaidis G, Xinarianos G, Gosney JR, et al. UHRF1-mediated tumor suppressor gene inactivation in nonsmall cell lung cancer. Cancer. 2010; 117:1027–1037. [PubMed: 21351083]
13. Wang F, Yang YZ, Shi CZ, Zhang P, Moyer MP, Zhang HZ, et al. UHRF1 promotes cell growth and metastasis through repression of p16(ink4a) in colorectal cancer. Ann Surg Oncol. 2012; 19:2753–2762. [PubMed: 22219067]
14. Du Z, Song J, Wang Y, Zhao Y, Guda K, Yang S, et al. DNMT1 stability is regulated by proteins coordinating deubiquitination and acetylation-driven ubiquitination. Sci Signal. 2010; 3:ra80. [PubMed: 21045206]
15. Sabatino L, Fucci A, Pancione M, Carafa V, Nebbioso A, Pistore C, et al. UHRF1 coordinates peroxisome proliferator activated receptor gamma (PPARG) epigenetic silencing and mediates colorectal cancer progression. Oncogene. (e-pub ahead of print 30 January 2012;). 10.1038/onc.2012.3
16. Jenkins Y, Markovtsov V, Lang W, Sharma P, Pearsall D, Warner J, et al. Critical role of the ubiquitin ligase activity of UHRF1, a nuclear RING finger protein, in tumor cell growth. Mol Biol Cell. 2005; 16:5621–5629. [PubMed: 16195352]
17. Babbio F, Pistore C, Curti L, Castiglioni I, Kunderfranco P, Brino L, et al. The SRA protein UHRF1 promotes epigenetic crosstalks and is involved in prostate cancer progression. Oncogene. (e-pub ahead of print 13 February 2012;). 10.1038/onc.2011.641
18. Unoki M, Kelly JD, Neal DE, Ponder BA, Nakamura Y, Hamamoto R. UHRF1 is a novel molecular marker for diagnosis and the prognosis of bladder cancer. Br J Cancer. 2009; 101:98–105. [PubMed: 19491893]
19. Yang GL, Zhang LH, Bo JJ, Chen HG, Cao M, Liu DM, et al. UHRF1 is associated with tumor recurrence in non-muscle-invasive bladder cancer. Med Oncol. 2011; 29:842–847. [PubMed: 21611839]
20. Un F, Qi C, Prosser M, Wang N, Zhou B, Bronner C, et al. Modulating ICBP90 to suppress human ribonucleotide reductase M2 induction restores sensitivity to hydroxyurea cytotoxicity. Anticancer Res. 2006; 26:2761–2767. [PubMed: 16886595]
21. Jin W, Chen L, Chen Y, Xu SG, Di GH, Yin WJ, et al. UHRF1 is associated with epigenetic silencing of BRCA1 in sporadic breast cancer. Breast Cancer Res Treat. 2010; 123:359–373. [PubMed: 19943104]
22. Alhosin M, Sharif T, Mousli M, Etienne-Selloum N, Fuhrmann G, Schni-Kerth VB, et al. Down-regulation of UHRF1, associated with re-expression of tumor suppressor genes, is a common feature of natural compounds exhibiting anti-cancer properties. J Exp Clin Cancer Res. 2011; 30:41. [PubMed: 21496237]
23. Jeanblanc M, Mousli M, Hopfner R, Bathami K, Martinet N, Abbady AQ, et al. The retinoblastoma gene and its product are targeted by ICBP90: a key mechanism in the G1/S transition during the cell cycle. Oncogene. 2005; 24:7337–7345. [PubMed: 16007129]
24. Kim JK, Esteve PO, Jacobsen SE, Pradhan S. UHRF1 binds G9a and participates in p21 transcriptional regulation in mammalian cells. Nucleic Acids Res. 2009; 37:493–505. [PubMed: 19056828]
25. de The H, Chomienne C, Lanotte M, Degos L, Dejean A. The t(15;17) translocation of acute promyelocytic leukaemia fuses the retinoic acid receptor alpha gene to a novel transcribed locus. Nature. 1990; 347:558–561. [PubMed: 2170850]
26. Reineke EL, Kao HY. Targeting promyelocytic leukemia protein: a means to regulating PML nuclear bodies. Int J Biol Sci. 2009; 5:366–376. [PubMed: 19471587]
27. Reineke EL, Liu Y, Kao HY. Promyelocytic leukemia protein controls cell migration in response to hydrogen peroxide and insulin-like growth factor-1. J Biol Chem. 2010; 285:9485–9492. [PubMed: 20100838]

28. Gurrieri C, Capodieci P, Bernardi R, Scaglioni PP, Nafa K, Rush LJ, et al. Loss of the tumor suppressor PML in human cancers of multiple histologic origins. J Natl Cancer Inst. 2004; 96:269–279. [PubMed: 14970276]
29. Fanelli M, Fantozzi A, De Luca P, Caprodossi S, Matsuzawa S, Lazar MA, et al. The coiled-coil domain is the structural determinant for mammalian homologues of Drosophila Sina-mediated degradation of promyelocytic leukemia protein and other tripartite motif proteins by the proteasome. J Biol Chem. 2004; 279:5374–5379. [PubMed: 14645235]
30. Boutell C, Canning M, Orr A, Everett RD. Reciprocal activities between herpes simplex virus type 1 regulatory protein ICP0, a ubiquitin E3 ligase, and ubiquitin-specific protease USP7. J Virol. 2005; 79:12342–12354. [PubMed: 16160161]
31. Louria-Hayon I, Alsheich-Bartok O, Levav-Cohen Y, Silberman I, Berger M, Grossman T, et al. E6AP promotes the degradation of the PML tumor suppressor. Cell Death Differ. 2009; 16:1156–1166. [PubMed: 19325566]
32. Yuan WC, Lee YR, Huang SF, Lin YM, Chen TY, Chung HC, et al. A Cullin3-KLHL20 Ubiquitin ligase-dependent pathway targets PML to potentiate HIF-1 signaling and prostate cancer progression. Cancer Cell. 2011; 20:214–228. [PubMed: 21840486]
33. Tatham MH, Geoffroy MC, Shen L, Plechanovova A, Hattersley N, Jaffray EG, et al. RNF4 is a poly-SUMO-specific E3 ubiquitin ligase required for arsenic-induced PML degradation. Nat Cell Biol. 2008; 10:538–546. [PubMed: 18408734]
34. Lallemand-Breitenbach V, Jeanne M, Benhenda S, Nasr R, Lei M, Peres L, et al. Arsenic degrades PML or PML-RARalpha through a SUMO-triggered RNF4/ubiquitin-mediated pathway. Nat Cell Biol. 2008; 10:547–555. [PubMed: 18408733]
35. Reineke EL, Lam M, Liu Q, Liu Y, Stanya KJ, Chang KS, et al. Degradation of the tumor suppressor PML by Pin1 contributes to the cancer phenotype of breast cancer MDA-MB-231 cells. Mol Cell Biol. 2008; 28:997–1006. [PubMed: 18039859]
36. Jensen K, Shiels C, Freemont PS. PML protein isoforms and the RBCC/TRIM motif. Oncogene. 2001; 20:7223–7233. [PubMed: 11704850]
37. Felle M, Joppien S, Nemeth A, Diermeier S, Thalhammer V, Dobner T, et al. The USP7/Dnmt1 complex stimulates the DNA methylation activity of Dnmt1 and regulates the stability of UHRF1. Nucleic Acids Res. 2011; 39:8355–8365. [PubMed: 21745816]
38. Ma H, Chen H, Guo X, Wang Z, Sowa ME, Zheng L, et al. M phase phosphorylation of the epigenetic regulator UHRF1 regulates its physical association with the deubiquitylase USP7 and stability. Proc Natl Acad Sci USA. 2012; 109:4828–4833. [PubMed: 22411829]
39. van Wijk SJ, de Vries SJ, Kemmeren P, Huang A, Boelens R, Bonvin AM, et al. A comprehensive framework of E2-RING E3 interactions of the human ubiquitin-proteasome system. Mol Syst Biol. 2009; 5:295. [PubMed: 19690564]
40. Rajakumara E, Wang Z, Ma H, Hu L, Chen H, Lin Y, et al. PHD finger recognition of unmodified histone H3R2 links UHRF1 to regulation of euchromatic gene expression. Mol Cell. 2011; 43:275–284. [PubMed: 21777816]
41. Nady N, Lemak A, Walker JR, Avvakumov GV, Kareta MS, Achour M, et al. Recognition of multivalent histone states associated with heterochromatin by UHRF1. J Biol Chem. 2011; 286:24300–24311. [PubMed: 21489993]
42. Wang DY, Done SJ, McCready DR, Boerner S, Kulkarni S, Leong WL. A new gene expression signature, the ClinicoMolecular Triad Classification, may improve prediction and prognostication of breast cancer at the time of diagnosis. Breast Cancer Res. 2011; 13:R92. [PubMed: 21939527]
43. Unoki M, Brunet J, Mousli M. Drug discovery targeting epigenetic codes: the great potential of UHRF1, which links DNA methylation and histone modifications, as a drug target in cancers and toxoplasmosis. Biochem Pharmacol. 2009; 78:1279–1288. [PubMed: 19501055]
44. Terris B, Baldin V, Dubois S, Degott C, Flejou JF, Henin D, et al. PML nuclear bodies are general targets for inflammation and cell proliferation. Cancer Res. 1995; 55:1590–1597. [PubMed: 7882370]
45. Gao C, Cheng X, Lam M, Liu Y, Liu Q, Chang KS, et al. Signal-dependent regulation of transcription by histone deacetylase 7 involves recruitment to promyelocytic leukemia protein nuclear bodies. Mol Biol Cell. 2008; 19:3020–3027. [PubMed: 18463162]

46. Cheng X, Liu Y, Chu H, Kao HY. Promyelocytic leukemia protein (PML) regulates endothelial cell network formation and migration in response to tumor necrosis factor alpha (TNFalpha) and interferon alpha (IFNalpha). J Biol Chem. 2012; 287:23356–23367. [PubMed: 22589541]
47. Sarkari F, Wang X, Nguyen T, Frappier L. The herpesvirus associated ubiquitin specific protease, USP7, is a negative regulator of PML proteins and PML nuclear bodies. PLoS One. 2011; 6:e16598. [PubMed: 21305000]
48. Canning M, Boutell C, Parkinson J, Everett RD. A RING finger ubiquitin ligase is protected from autocatalyzed ubiquitination and degradation by binding to ubiquitin-specific protease USP7. J Biol Chem. 2004; 279:38160–38168. [PubMed: 15247261]
49. Pearson M, Carbone R, Sebastiani C, Cioce M, Fagioli M, Saito S, et al. PML regulates p53 acetylation and premature senescence induced by oncogenic Ras. Nature. 2000; 406:207–210. [PubMed: 10910364]
50. Hofmann TG, Moller A, Sirma H, Zentgraf H, Taya Y, Droge W, et al. Regulation of p53 activity by its interaction with homeodomain-interacting protein kinase-2. Nat Cell Biol. 2002; 4:1–10. [PubMed: 11740489]
51. Lim JH, Liu Y, Reineke E, Kao HY. Mitogen-activated protein kinase extracellular signal-regulated kinase 2 phosphorylates and promotes Pin1 protein-dependent promyelocytic leukemia protein turnover. J Biol Chem. 2011; 286:44403–44411. [PubMed: 22033920]
52. Khurana S, Chakraborty S, Cheng X, Su YT, Kao HY. The actin-binding protein, actinin alpha 4 (ACTN4), is a nuclear receptor coactivator that promotes proliferation of MCF-7 breast cancer cells. J Biol Chem. 2011; 286:1850–1859. [PubMed: 21078666]
53. Leng RP, Lin Y, Ma W, Wu H, Lemmers B, Chung S, et al. Pirh2, a p53-induced ubiquitin-protein ligase, promotes p53 degradation. Cell. 2003; 112:779–791. [PubMed: 12654245]

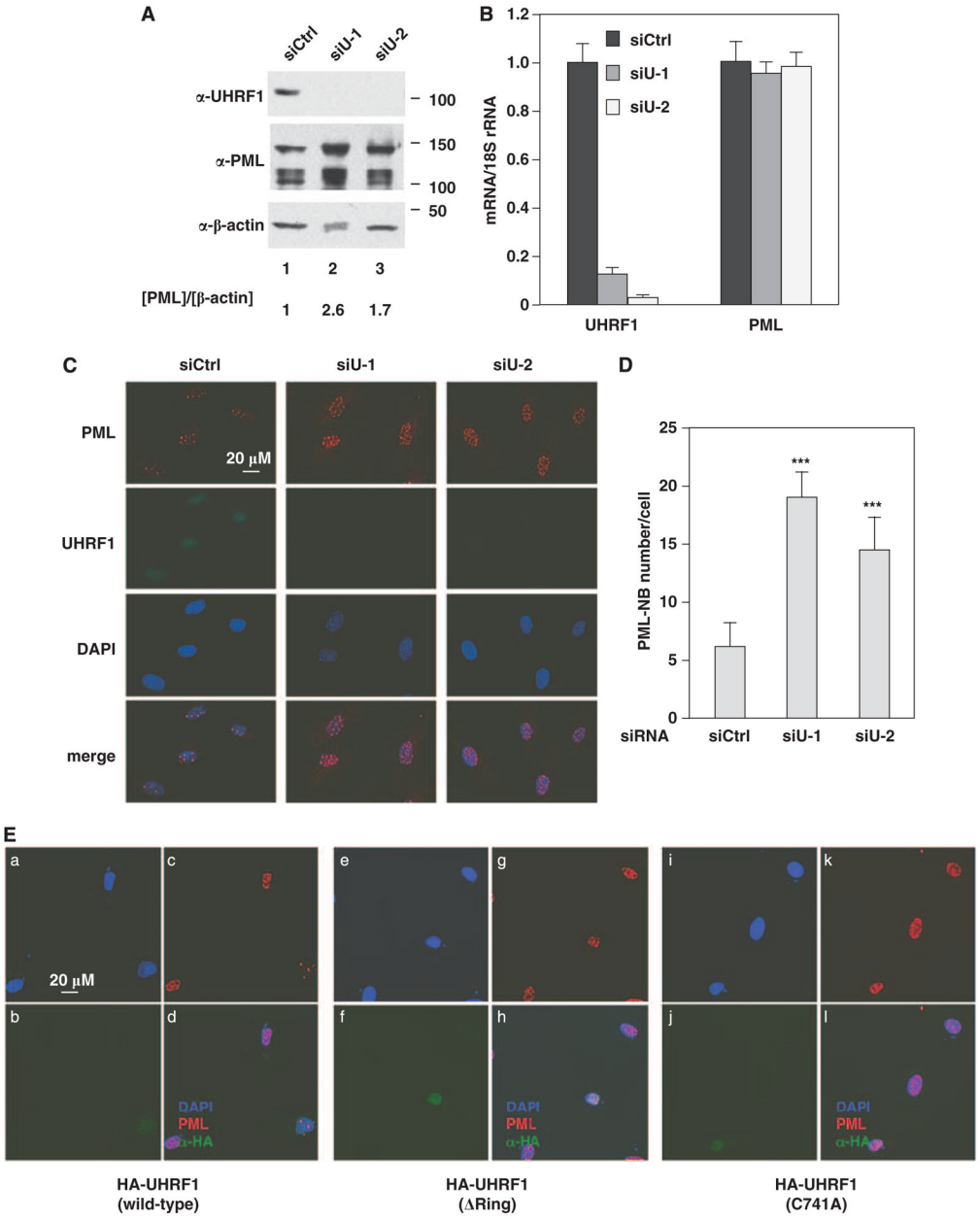

Figure 1.

UHRF1 negatively regulates PML protein accumulation in HUVECs. (**A**, **B**) HUVECs were transfected with scramble or two different UHRF1 siRNA for 72 h. An aliquot of cells were used to analyze protein (**A**) or mRNA (**B**) levels. (**A**) Whole-cell lysates prepared from HUVECs transfected with scramble or two different UHRF1 siRNA were analyzed by immunoblotting with anti-UHRF1, anti-PML and anti-β-actin antibodies. β-Actin served as a loading control. The intensity of the bands was quantified by ImageJ and normalized to β-actin, and the relative PML protein levels were presented as [PML]/[β-actin]. (**B**) Total RNA was isolated and analyzed by reverse transcriptase–PCR (RT–PCR) and quantitative RT–PCR to analyze PML expression. 18S RNA was used as an internal control. There was no significant change in 18S RNA observed between scramble and UHRF1 siRNA transfected cells. (**C**) HUVECs were transfected with indicated siRNAs for 72 h. Cells were

immunostained with anti-PML and anti-UHRF1 antibodies, and images were taken by fluorescence microscopy (original magnification ×200). (**D**) Numbers of PML nuclear bodies (NBs) in each cell were counted. Over 100 cells in duplicated experiments were counted and presented as means±s.d. Unpaired two-tail *t*-tests (***$P<0.001$) were used for statistical analyses. (**E**) HUVECs were transfected with HA-UHRF1 (wild-type) (a–d), or HA-UHRF1 (ΔRing) (e, h) or HA-UHRF1 (C741A) (i–l) for 48 h. Cells were immunostained with anti-PML and anti-HA antibodies and images were taken by fluorescence microscopy. DAPI (4,6-diamidino-2-phenylindole) was used to indicate nuclei.

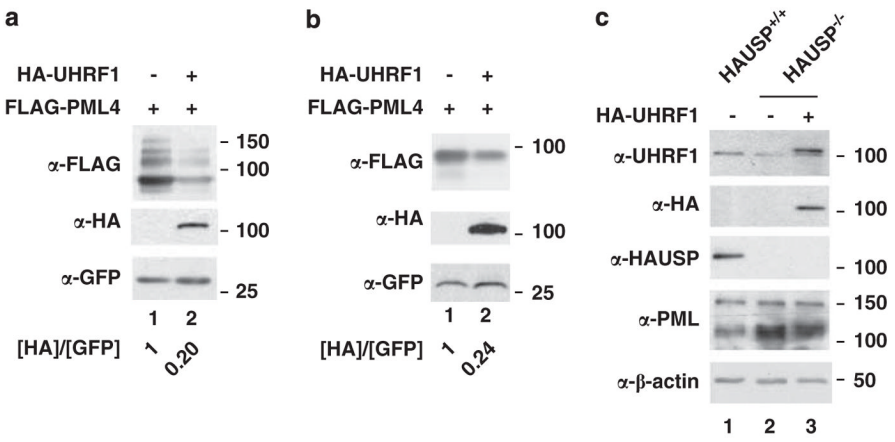

Figure 2.

Ectopic overexpression of UHRF1 decreased PML protein levels in mammalian cells. (**a**, **b**) HEK 293 cells (**a**) or HeLa cells (**b**) were co-transfected with HA-UHRF1, FLAG-PML4 and GFP for 48 h. Cells were lysed and analyzed by immunoblotting with anti-FLAG, anti-HA and anti-GFP antibodies. GFP served as a transfection and loading control. (**c**) The effect of overexpressing HA-UHRF1 on endogenous PML protein levels. Wild-type DLD1 cells were transfected with HA empty vector, whereas HAUSP knockout DLD1 cells were transfected with HA empty vector or HA-UHRF1. Cell lysates were analyzed by immunoblotting using the indicated antibodies.

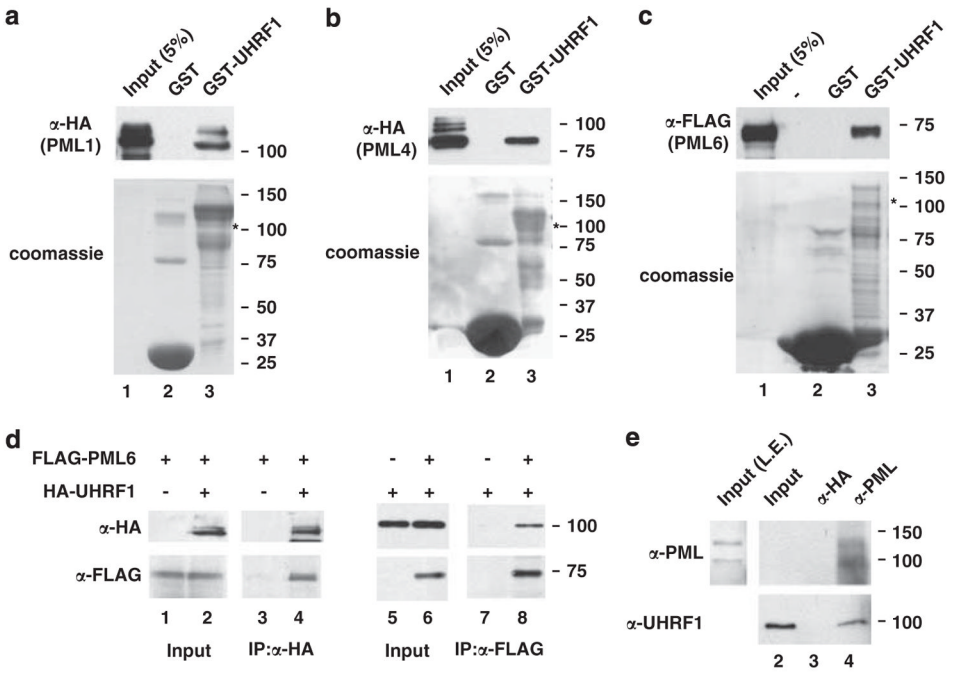

Figure 3.

UHRF1 interacts with PML. (**a**–**c**) HEK 293 cells were transfected with HA- PML1 (**a**), PML4 (**b**) or PML6 (**c**). Whole-cell lysates were prepared and incubated with GST, or GST-UHRF1 for 1 h. The pull-down fractions were analyzed by immunoblotting with anti-HA antibodies. Full-length GST-UHRF1 is marked as asterisk. (**d**) HEK 293 cells were transfected with FLAG-PML with or without HA-UHRF1, and whole-cell lysates were immunoprecipitated with anti-HA beads (lanes 3 and 4) or anti-FLAG conjugated beads (lanes 7 and 8). The immune pellets were analyzed by western blotting with anti-FLAG and anti-HA antibodies. (**e**) Whole-cell lysates from HUVECs were prepared and immunoprecipitated with anti-HA (lane 3) or anti-PML (lane 4) antibodies. The immune pellets were separated by SDS–PAGE, and immunoblotting was performed with anti-UHRF1 and anti-PML antibodies. A total of 2.5% of input (lanes 1 and 2) was loaded. LE, longer exposure.

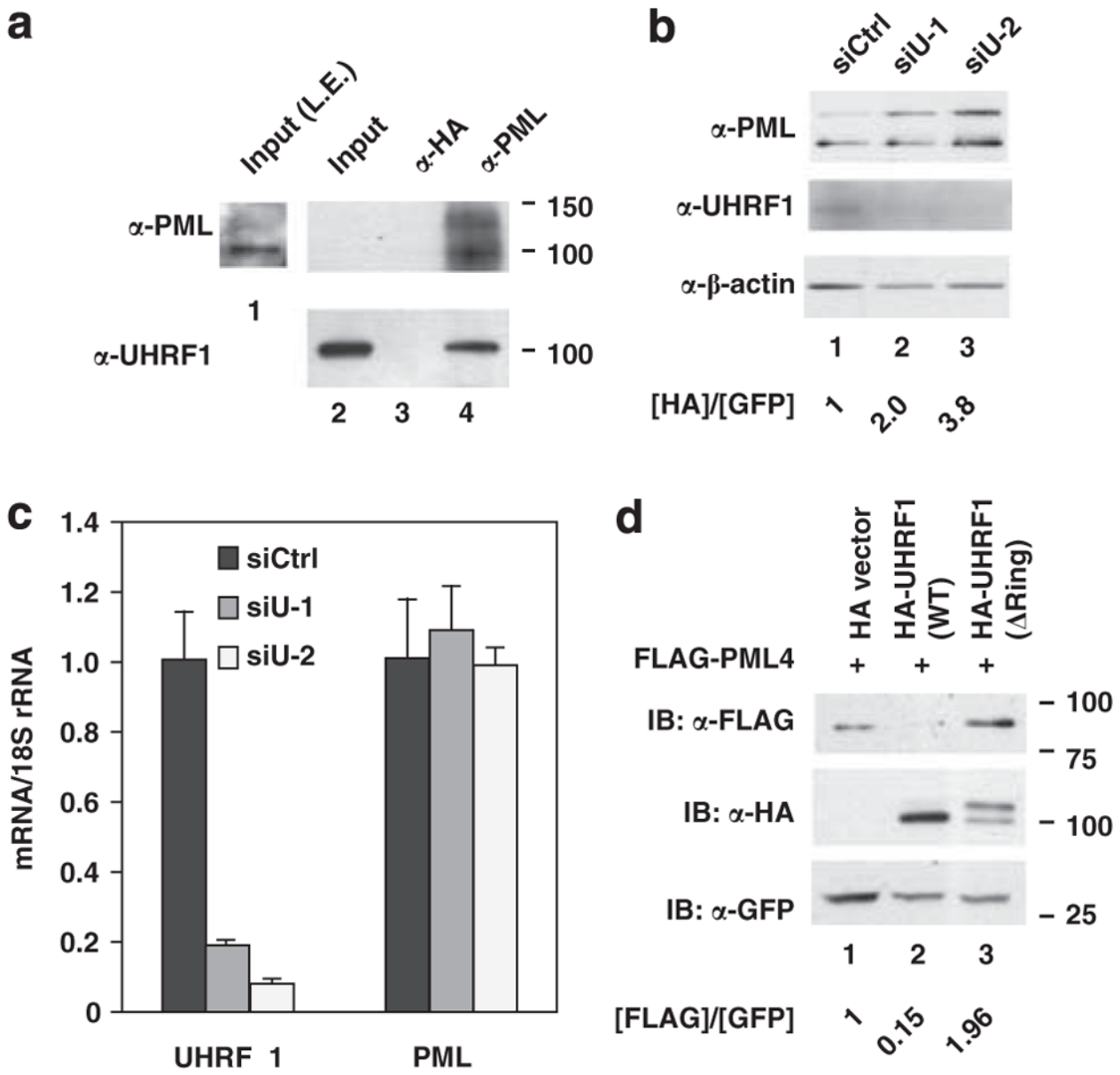

Figure 4.

UHRF1 negatively regulates PML protein accumulation in PC3 prostate cancer cells. (**a**) Endogenous UHRF1 and PML interact. Whole-cell extracts prepared from PC3 cells were immunoprecipitated with anti-PML antibodies followed by immunoblotting with anti-PML and anti-UHRF1 antibodies. A total of 5% of input was loaded in lane 1. LE, longer exposure. (**b**) Knockdown of UHRF1 increases PML protein levels. (**c**) Knockdown of UHRF1 does not significantly alter PML mRNA accumulation. (**d**) The UHRF1 E3 ligase activity is essential for UHRF1-mediated downregulation of PML protein levels. PC3 cells were transiently transfected with FLAG-PML4, GFP and HA vector, HA-tagged wild-type, ΔRing mutant UHRF1. Whole-cell extracts were analyzed by immunoblotting with GFP, anti-HA and anti-FLAG antibodies.

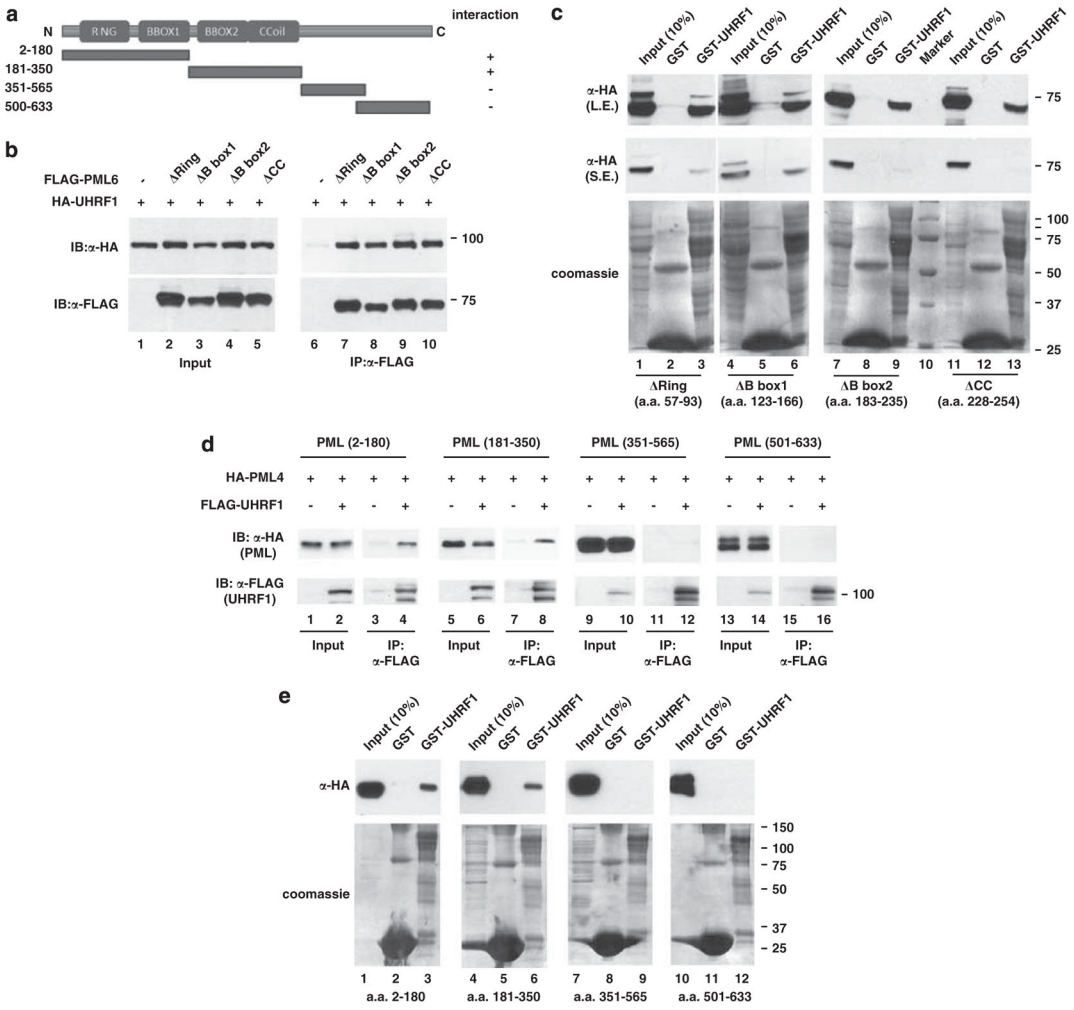

Figure 5.

Mapping UHRF1 interacting domain in PML. (**a**) A summary of domain mapping results. PML possesses Ring, B-box 1, B-box 2 and CC domains. The summary of domain mapping study is based on GST pull-down and coimmunoprecipitation experiments. (**b**) Cells were transiently transfected with the indicated plasmids, cell extracts prepared and immunoprecipitated with anti-FLAG antibodies. The immune pellets were immunoblotted with anti-FLAG or anti-HA antibodies. (**c**) Immobilized, purified, GST-UHRF1 was incubated with cell extracts expressing HA-tagged PML deletion mutants followed by immunoblotting with anti-HA antibodies. LE, longer exposure. SE, short exposure. (**d**, **e**) The experiments were performed as described in (**b** and **c**) respectively, except that a different set of PML expression constructs were used. a.a., amino acid.

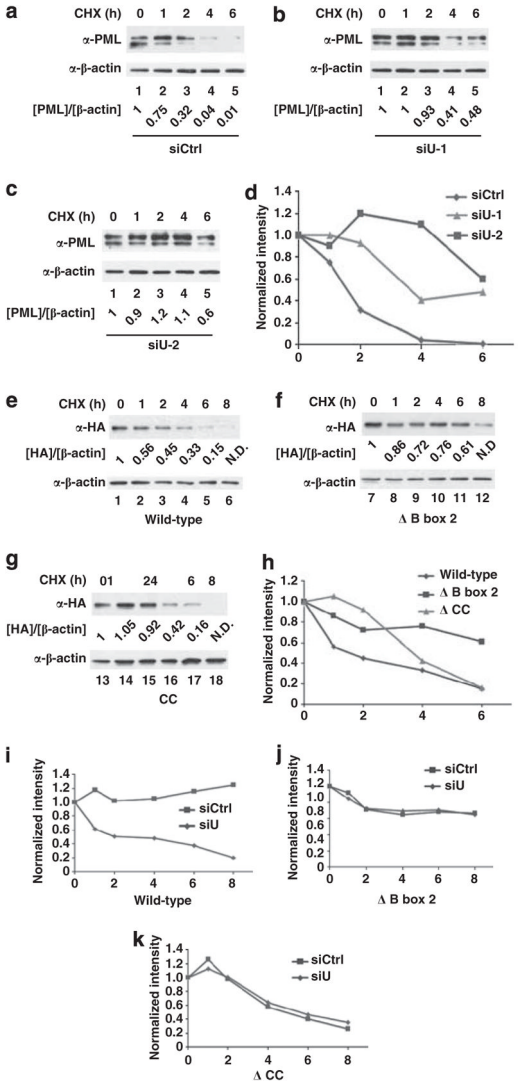

Figure 6.

Knockdown of UHRF1 prolongs PML protein half-life. The half-life of endogenous (HUVECs; **a**–**d**) and transfected PML (HeLa cells; **e**–**k**). (**a**–**d**) HUVECs were transfected with a nontargeting siRNA (**a**) or two independent UHRF1 siRNAs (**b**, **c**) and the half-life of endogenous PML was determined as described in the Materials and methods. (**d**) Quantification of the immunoblots from (**a**–**c**). Knockdown efficiency of UHRF1 is shown in Supplementary Figure 3. (**e**–**h**) The half-life of wild-type and mutant PML. HeLa cells were transiently transfected with wild-type PML (**e**), PML (ΔB-box 2) (**f**) or PML (ΔCC) (**g**) and the half-life of transfected PML was determined as described in the Materials and methods. (**h**) Quantification of the immunoblots from (**e**–**g**). (**i**–**k**) The half-life of transfected wild-type or mutant PML in UHRF1 knockdown cells. HeLa cells were transiently transfected with a nontargeting siRNA or a UHRF1 siRNA. Cells were trypsinized and equal numbers of cells were transiently transfected with wild-type PML (**i**), PML (ΔB-box 2) (**j**) or PML (ΔCC) (**k**) expression plasmid. UHRF1 knockdown efficiency and the immunoblots are shown in Supplementary Figure 4. CHX, cycloheximide. ND, no detectable.

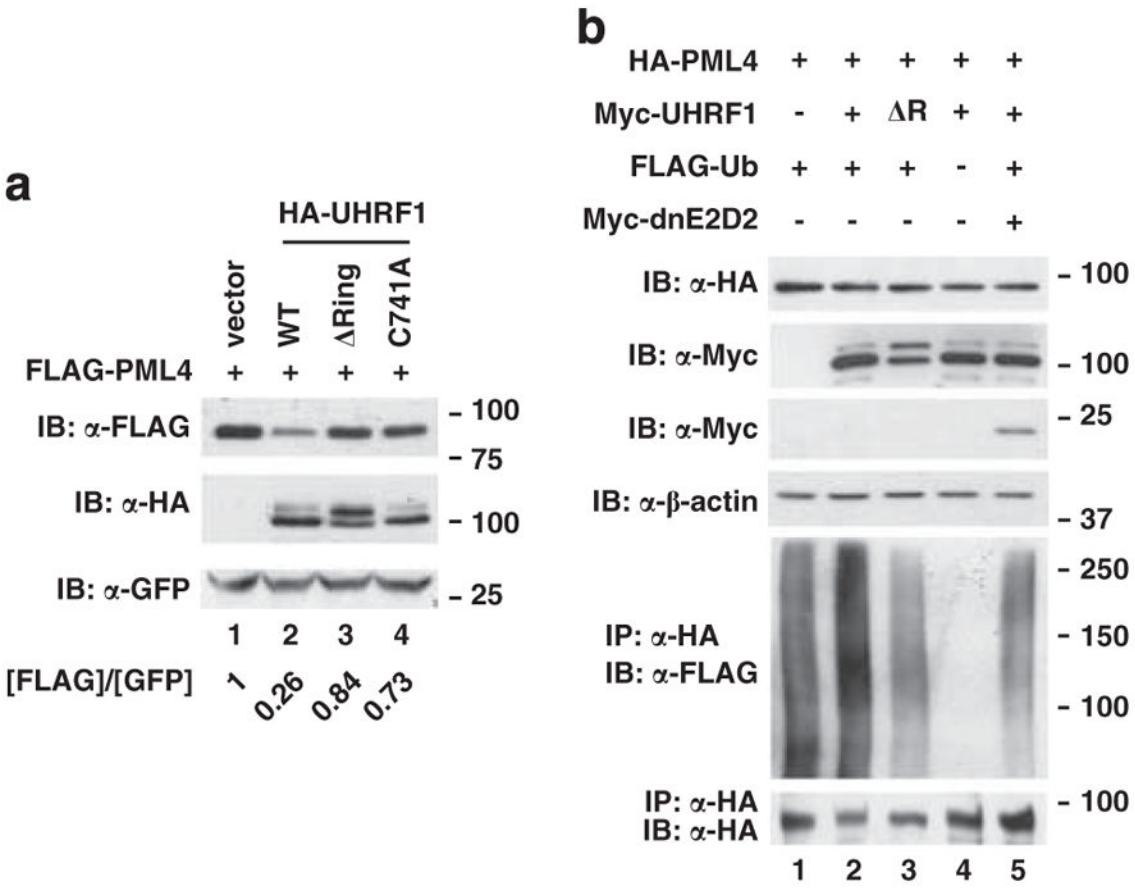

Figure 7.

The RING domain is essential for UHRF1-mediated PML ubiquitination and degradation. (**a**) HEK 293 T cells were co-transfected with HA-PML4 and GFP in the presence of wild-type UHRF1 (lane 1), an empty vector (lane 2), a RING deletion mutant, ΔRING (lane 3) or a point mutant C741A (lane 4). Whole-cell lysates were analyzed by immunoblotting with the indicated antibodies. Note that the full-length UHRF1 has two bands. The slower migrating band is likely a modified form of UHRF1 and its intensity is much lower than the faster migrating species. The ΔRING mutant also has two bands. Interestingly, the intensity of the slower migrating band is slightly lower than that of the faster migrating band. (**b**) UHRF1 and E2D2 promote PML polyubiquitination. HEK 293 cells were co-transfected with indicated plasmids. Whole-cell extracts were prepared and immunoprecipitated with anti-HA antibodies followed by immunoblotting with anti-FLAG or anti-HA antibodies.

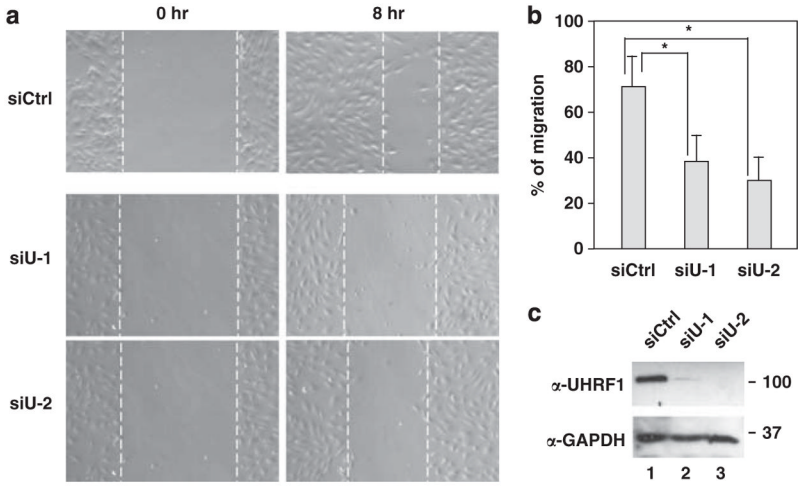

Figure 8.

Knockdown of UHRF1 inhibits HUVEC migration. (**a**) Representative images of wound-healing assays. HUVECs were transiently transfected with a nontargeting or two different UHRF1 siRNAs. At 60 h after transfection, wound-healing assays were performed as described in the Materials and methods. (**b**) Statistical analyses of wound-healing assays. (**c**) UHRF1 is efficiently knocked down by siRNAs. Whole-cell extracts were prepared from HUVECs 60 h after siRNA transfection. Immunoblotting was performed to determine UHRF1 knockdown efficiency. Wound-healing assays were performed as described in the Materials and methods. Unpaired two-tail *t*-tests (**P*<0.01) were used for statistical analyses.

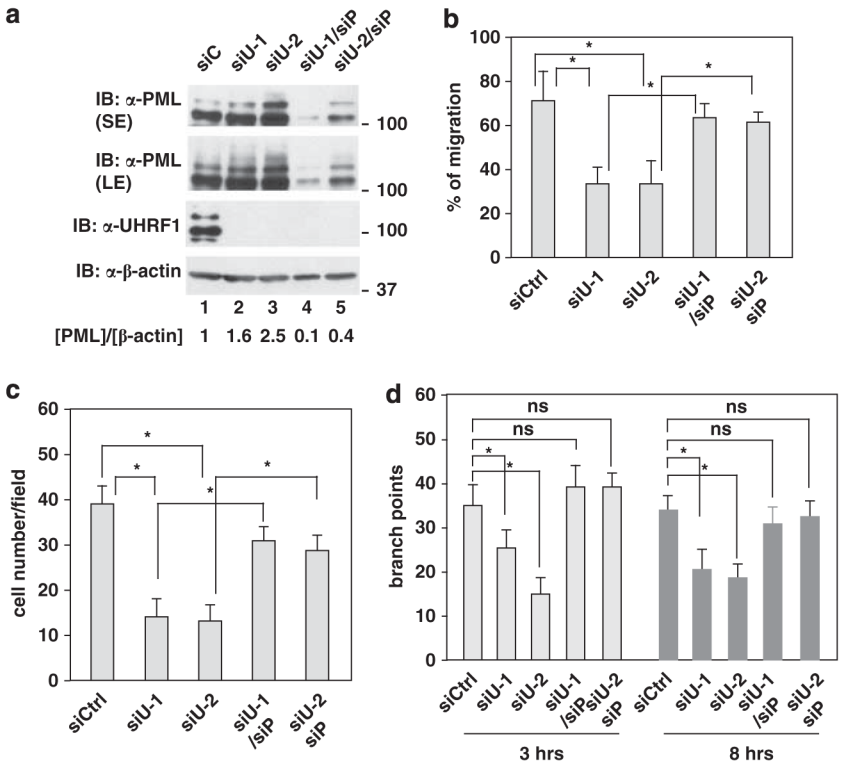

Figure 9.

Knockdown of PML alleviates UHRF1 depletion-mediated inhibition of HUVEC migration, invasion and capillary tube formation. (**a**) HUVECs were transiently transfected with the siRNAs targeting UHRF1 and/or PML. An aliquot of the cells was subjected to immunoblotting with anti-UHRF1 and anti-PML antibodies. LE, longer exposure; SE, shorter exposure. The intensities of the bands were quantified by ImageJ and normalized to β-actin, which presented as [PML]/[β-actin]. An aliquot of the cells was seeded 60 h after knockdown followed by wound-healing (**b**), transwell migration (**c**) or capillary tube formation (**d**) assays as described in the Materials and methods. Unpaired two-tail *t*-tests (**P*<0.01; ns, not significant) were used for statistical analyses.